



Stability and Performance Analysis of Active Topological Non-hermitian Metastructures

Danilo Braghini¹, Juan F. Camino¹, José R.F. Arruda¹

¹*School of Mechanical Engineering, University of Campinas
R. Mendeleev, 200 - Cidade Universitária, 13083-860, Campinas, Brazil
braghinidan@gmail.com*

Abstract.

Metamaterials can be divided into passive and active types, with the latter incorporating programmable devices in their design. While active metamaterials promise resilience against manufacturing inconsistencies and defects, a notable gap exists in the current literature regarding metastructure stability and performance. Historically, the phenomena linked to non-Hermitian systems were investigated in quantum mechanics, but recent breakthroughs have translated them into classical mechanics. This research investigates the stability of active metamaterials through numerical simulations of a one-dimensional structure, wherein each unit cell showcases periodic feedback interactions. Stability limits for different feedback laws are determined. Central to this investigation is the relationship between closed-loop stability and directional propagation driven by the topological skin effect. This analysis entails exploring how distinct control law strategies affect stability and performance.

Keywords: non-Hermitian systems, topological modes, skin effect, stability analysis, metamaterials

1 Introduction

Applications of periodic systems in mechanical engineering involve the design of phononic crystals and acoustic metamaterials [1, 2]. In this context, non-Hermitian systems [3] have been investigated for macroscopic elastic/acoustic metamaterials. Among their key properties, these systems primarily exhibit large non-reciprocity associated with directional wave amplification and attenuation. Topological modes associated with the Non-Hermitian Skin Effect (NHSE), where many bulk modes of a 1D system become localized at a boundary, have been predicted and experimentally observed [4–9]. These works illustrate the NHSE, named in analogy to the electrical conductor effect of the same name, not found in Hermitian (conservative) counterparts. The NHSE has been used in the design of active functional metamaterials such as sensors [10], non-reciprocal robots using feedback loops [11, 12], and control of filaments and membranes in biological systems using feedforward loops [13]. In practice, the NHSE manifests as topological modes localized at finite domain boundaries and can be predicted by momentum space topology.

This paper employs simple lattice models (lumped-parameter systems) of non-Hermitian, non-reciprocal metamaterials. The dispersion diagrams of this metamaterial and the implications of NHSE on this type of finite structure have already been demonstrated in a previous work [14], in which, spectral elements were used to show that this periodic system exhibits the wave behavior associated with a non-trivial topology on the reciprocal space. The winding number, a topological invariant, was determined by directly observing the dispersion relation. It was used to predict the localization of the skin modes of the finite system, derived from truncating the metamaterial at both ends under arbitrary boundary conditions. Finite element models were used to compute the eigenmodes (skin modes) of this flexible structure [15]. The non-reciprocal wave propagation due to the NHSE was verified by the time domain response of the system to a transient external force.

Active mechanical systems utilizing feedback loops have been extensively explored in recent literature [8, 9, 11, 12, 16–18]. However, the investigation of periodic structures with feedback interactions is still in its earlier stages, demanding further understanding of their fundamental properties and practical applicability. This paper provides a preliminary examination of the stability and performance analysis of metastructures tailored to realize

the NHSE. First, Section 2 presents the model of the structure under investigation. Section 3 offers an attempt to quantify the NHSE in these structures using their frequency response, also highlighting the relationship with the H_2 norm, a recognized performance metric. Section 4 delves into the effects of proportional and derivative feedback strategies on the closed-loop system's stability, with a noteworthy observation concerning the minimal influence of the damping factor. Finally, Section 5 concludes by summarizing the primary contributions and findings.

2 The lumped parameter model

The metamaterial under study is a one-dimensional classical mechanical waveguide exhibiting both non-Hermitian and non-reciprocal properties. This behavior is achieved by periodically applying feedback interactions in an asymmetrical fashion. The associated system has N degrees of freedom, represented as $q_i(t)$, and features boundary masses fixed to rigid walls on either ends, as shown in Fig. 1.

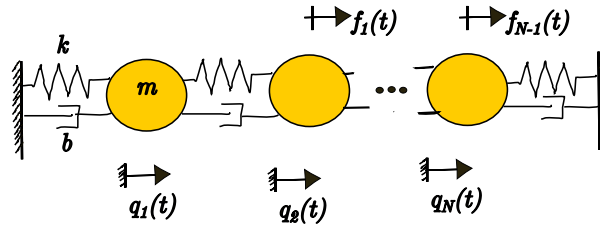


Figure 1: Active metastructure model with feedback forces.

In this work, the system parameters are set to $N = 7$ (masses), $m = 1$ kg and $k = 10$ N/m. The effects of varying the damping factor b and the feedback gains are examined. For this system, the expression for the feedback law $f_i(t)$ is defined as $f_i(t) = \mathcal{G}(q_{i+1}(t) - q_i(t))$, for $1 \leq i \leq N - 1$, where \mathcal{G} denotes an operation. For pure proportional feedback, $\mathcal{G} = g_p$ acts as a constant. Whereas for derivative feedback, the time derivative operation is defined as $\mathcal{G} = g_d \text{d}/\text{d}t$.

When using the same value for all the masses, the unit cell is constituted of a single mass rather than two. As will be demonstrated in subsequent sections, this results in a frequency response function presenting a single passband, followed by a stop band that extends infinitely, rather than displaying two distinct bands separated by a band gap as highlighted in the literature.

3 A metric for the NHSE

As a first attempt to systematically assess the NHSE, we employ the frequency response of the flexible structure rather than its time response. The NHSE induces non-reciprocity in the forced harmonic response of the structure, specifically in the context of energy localization, a phenomenon previously reported in [8]. To quantify this, we introduce the metric A , defined by

$$A = | \|\hat{q}_N\|_{L_1} - \|\hat{q}_1\|_{L_1} | \quad (1)$$

where $\hat{q}_1(j\omega)$ and $\hat{q}_N(j\omega)$ are the *Fourier* transforms of the displacements $q_1(t)$ and $q_N(t)$ of the first and last masses, respectively, for a unit input force. The symbol $\|\cdot\|_{L_1}$ denotes the L_1 norm defined as

$$\|\hat{q}\|_{L_1} = \int_{-\infty}^{\infty} |\hat{q}(j\omega)| d\omega$$

It can be shown that the metric A represents the absolute value of the area between the curves $|\hat{q}_1(j\omega)|$ and $|\hat{q}_N(j\omega)|$, which correspond to the magnitude of their *Bode* plots.

From the *Cauchy-Schwartz* inequality, given two signals $f, g \in L_2$,

$$|\langle f, g \rangle_{L_2}| \leq \|f\|_{L_2} \|g\|_{L_2}. \quad (2)$$

Particularly, take $z = q_N - q_1$ the response to a unit input force. Then, $f = |\hat{z}|$ is the frequency response of the structure. Assuming, additionally, that the system is causal and asymptotically stable, as a consequence of the *Parseval* theorem and the symmetry of the *Fourier* transform of real signals.

$$f = \begin{cases} \geq 0, & -\omega_0 \leq \omega \leq \omega_0, \\ 0, & \text{otherwise,} \end{cases}$$

Moreover, take

$$g = \begin{cases} 1, & -\omega_0 \leq \omega \leq \omega_0, \\ 0, & \text{otherwise.} \end{cases}$$

Thus,

$$\|g\|_{L_2} = \sqrt{\left(\int_{-\infty}^{\infty} |g(j\omega)|^2 d\omega\right)} = \sqrt{2\omega_0}, \quad (3)$$

and

$$|\langle f, g \rangle_{L_2}| = \left| \int_{-\omega_0}^{\omega_0} f(j\omega) d\omega \right|,$$

which equals $\|f\|_{L_1} = \int_{-\omega_0}^{\omega_0} f(j\omega) d\omega$ since $f(j\omega) \geq 0 \quad \forall \omega \in \mathbb{R}$. Moreover, $f(j\omega) = |\hat{z}(j\omega)| = |\hat{q}_N(j\omega) - \hat{q}_1(j\omega)| \geq ||\hat{q}_N(j\omega)| - |\hat{q}_1(j\omega)||$. The last inequality can be proved $\forall z_1, z_2 \in \mathbb{C}$ and implies that

$$\begin{aligned} \|f\|_{L_1} &= \int_{-\infty}^{\infty} |\hat{q}_N(j\omega) - \hat{q}_1(j\omega)| d\omega \\ &\geq \int_{-\omega_0}^{\omega_0} ||\hat{q}_N(j\omega)| - |\hat{q}_1(j\omega)|| d\omega \\ &\geq \left| \int_{-\omega_0}^{\omega_0} |\hat{q}_N(j\omega)| d\omega - \int_{-\omega_0}^{\omega_0} |\hat{q}_1(j\omega)| d\omega \right| = A. \end{aligned} \quad (4)$$

Finally, recalling the definition of the H_2 norm of a linear system S with single input and single output z , [19], $\|S\|_{H_2} = \|\hat{z}\|_{L_2}$, and equations 2, 3, and 4 we have the following relation between the H_2 norm and the previously defined metric.

$$A \leq \|\hat{z}\|_{H_2} \sqrt{2\omega_0} \quad (5)$$

4 Results

The magnitudes of the Bode plots of the passive structure, for an external force \hat{F} applied at the middle (4th mass) and measured at the left (\hat{q}_1) and right (\hat{q}_7) ends, are identical. Consequently, $A = 0$. This is due to the symmetry of the structure. As the following subsections will demonstrate, by applying feedback, the system becomes non-reciprocal, which translates into asymmetric results. As previously highlighted in [8], the more pronounced the difference between the responses at the two ends (corresponding to higher values of A), the more evident the NHSE becomes in the time domain response of the structure.

A closed-loop dynamical system is asymptotically stable if and only if all of its poles have strictly negative real parts. In other words, the maximum real part of the poles, $\Re(\lambda)_{max}$, must be negative. As our simulations show that this condition is met only for gains $g \in I = (g_0, g_1)$. For these values, the maximum value of the metric A and the H_2 norm that can be achieved with each feedback strategy are computed. The optimal values are achieved with feedback gains $g_A, g_2 \in I$. In practice, however, small uncertainties in the system parameters may lead to pole variations. Thus, for robustness purposes, the poles should stay as far as possible from the imaginary axis.

4.1 Proportional Feedback

Table 1 shows that the interval I does not change considerably with damping, neither does A and the H_2 norm. Non-intuitively, this result seems to imply that the stability issue cannot be solved by adding viscous damping alone. Actually, the damping factor within its usual range for mechanical systems has little influence on the system dynamics. Moreover, both A and the H_2 norm assume higher values at the instability limits, which can be observed in the computed $\Re(\lambda)_{max}$ values. These results can be visualized in the plot of Fig. 5 (a). Note that the undamped structure ($b = 0$) has all eigenvalues on the imaginary axis. For a selected value of gain, Fig. 4 (a) shows a significant value of A , expressed by the asymmetric behavior of the frequency response.

Additionally, Fig. 2 shows the root locus of the closed-loop structure, i.e., how the poles of the closed-loop system evolve with varying values of feedback gain.

Table 1: Proportional feedback

| b | g_0 | g_1 | max A | g_A | max $ H_2 $ | g_2 | $\Re(\lambda)_{max}$ for $g_p = g_A$ |
|------|--------|-------|-------|--------|-------------|--------|--------------------------------------|
| 0 | $\#$ | $\#$ | $\#$ | $\#$ | $\#$ | $\#$ | 0 |
| 0.01 | -32.46 | 5.38 | 2.25 | -32.45 | 14.23 | -32.45 | -0.0007 |
| 0.05 | -33.08 | 5.58 | 2.09 | -33.07 | 14.06 | -33.07 | -0.0028 |
| 0.1 | -33.17 | 5.60 | 1.96 | -33.16 | 14.08 | -33.16 | -0.0053 |
| 0.2 | -33.24 | 5.62 | 1.50 | -33.22 | 12.91 | -33.23 | -0.0103 |
| 0.5 | -33.52 | 5.65 | 1.2 | -33.50 | 11.21 | -33.51 | -0.0232 |
| 1 | -34.38 | 5.73 | 1.28 | -34.37 | 12.50 | -34.37 | -0.0327 |
| 1.5 | -35.54 | 5.86 | 0.91 | -35.53 | 7.75 | -35.53 | -0.0251 |
| 2 | -36.72 | 6.03 | 0.79 | -36.70 | 11.43 | -36.71 | -0.0061 |

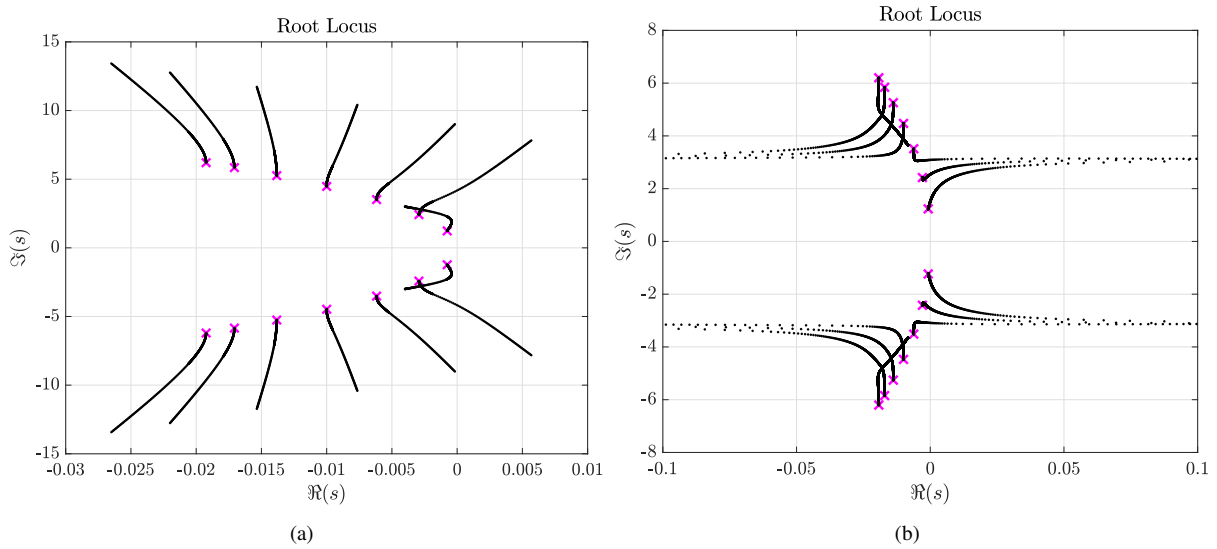


Figure 2: Root locus plot for the structure with $g_d = 0$, $b = 0.01$ and (a) $g_p < 0$ (b) $g_p > 0$. Magenta x denotes the poles of the open loop structure, with $g_p = g_d = 0$.

4.2 Derivative Feedback

Table 2 shows that, for any negative gain, the derivative feedback results in a stable closed-loop structure, as can be seen in Fig. 3. Again, both A and the H_2 norm show little or no influence of the damping factor. However, in Fig. 5 (b), the performance of the structure as a function of the feedback gain shows a very different behavior compared to the proportional feedback case. Now, both A and the H_2 norm have a maximum value inside I , although assuming considerably lower values. Also, for a selected gain value, Fig. 4 (b) shows again the asymmetric behavior of the frequency responses. Regarding stability, $\Re(\lambda)_{max}$ is considerably further away from the imaginary axis compared to the proportional feedback case.

5 Conclusion

It was shown that increasing the viscous damping has none or little effect on the dynamics of the investigated structure, while the feedback law can completely change its behavior. Further investigations are required and will be undertaken with the aim of designing a metastructure that maximizes A while maximizing $\Re(\lambda)_{max}$. Together with the analysis of the wave physics and using established topology tools, the NHSE must be confirmed on the designed structure. By addressing this problem, this work contributes by reducing the need for heuristic solutions in the design of active periodic metastructures exhibiting the non-Hermitian skin effect.

Table 2: Derivative feedback

| b | g_0 | g_1 | max A | g_A | max $ H_2 $ | g_2 | $\Re(\lambda)_{max}$ |
|------|-----------|-------|-------|--------|-------------|-------|----------------------|
| 0 | $-\infty$ | 0 | 0.05 | -10.93 | 0.12 | -2.44 | -0.1579 |
| 0.01 | $-\infty$ | 0 | 0.05 | -10.93 | 0.12 | -2.48 | -0.1582 |
| 0.05 | $-\infty$ | 0 | 0.05 | -10.91 | 0.11 | -2.64 | -0.1597 |
| 0.1 | $-\infty$ | 0 | 0.05 | -10.88 | 0.11 | -2.82 | -0.1615 |
| 0.2 | $-\infty$ | 0 | 0.05 | -10.84 | 0.10 | -3.16 | -0.1651 |
| 0.5 | $-\infty$ | 0 | 0.05 | -10.78 | 0.09 | -4.06 | -0.1758 |
| 1 | $-\infty$ | 0 | 0.05 | -10.84 | 0.08 | -5.16 | -0.1926 |
| 1.5 | $-\infty$ | 0 | 0.05 | -11.01 | 0.07 | -6.03 | -0.2077 |
| 2 | $-\infty$ | 0 | 0.05 | -11.27 | 0.06 | -6.82 | -0.2232 |

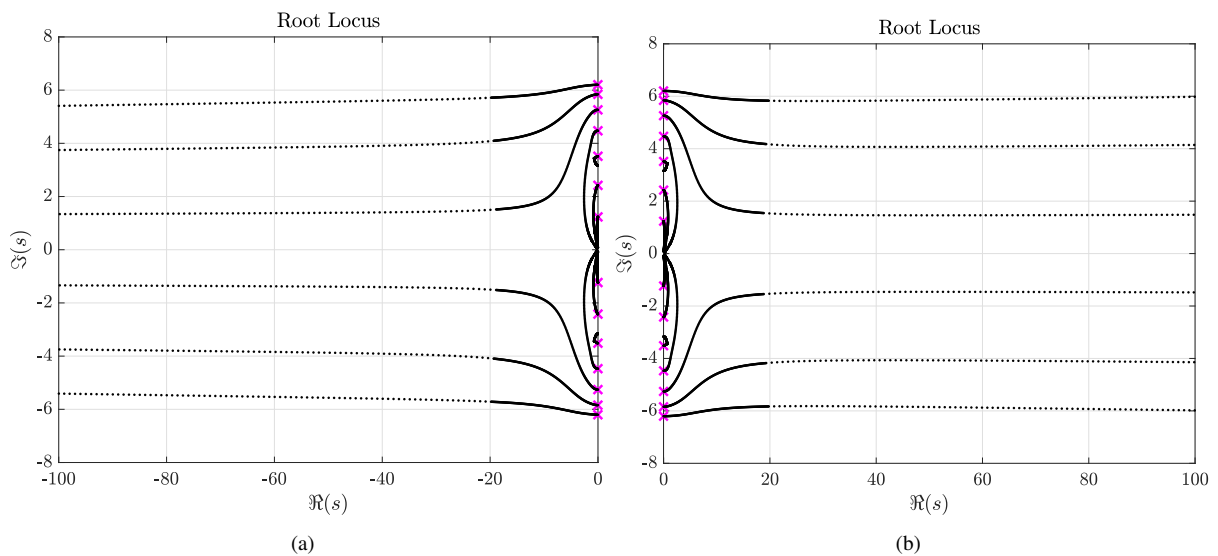


Figure 3: Root locus plot for the structure with $b = 0.01$, $g_p = 0$ and (a) $g_d < 0$ (b) $g_d > 0$.

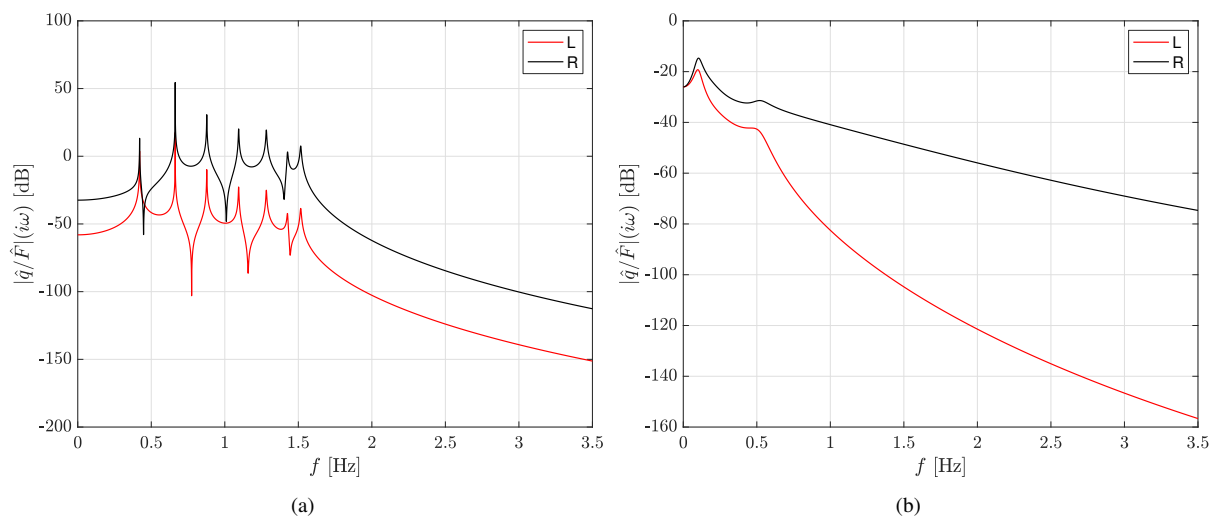


Figure 4: Frequency responses of the structure with: (a) $g_p = -30$ and $g_d = 0$. (b) $g_p = 0$ and $g_d = -11$.

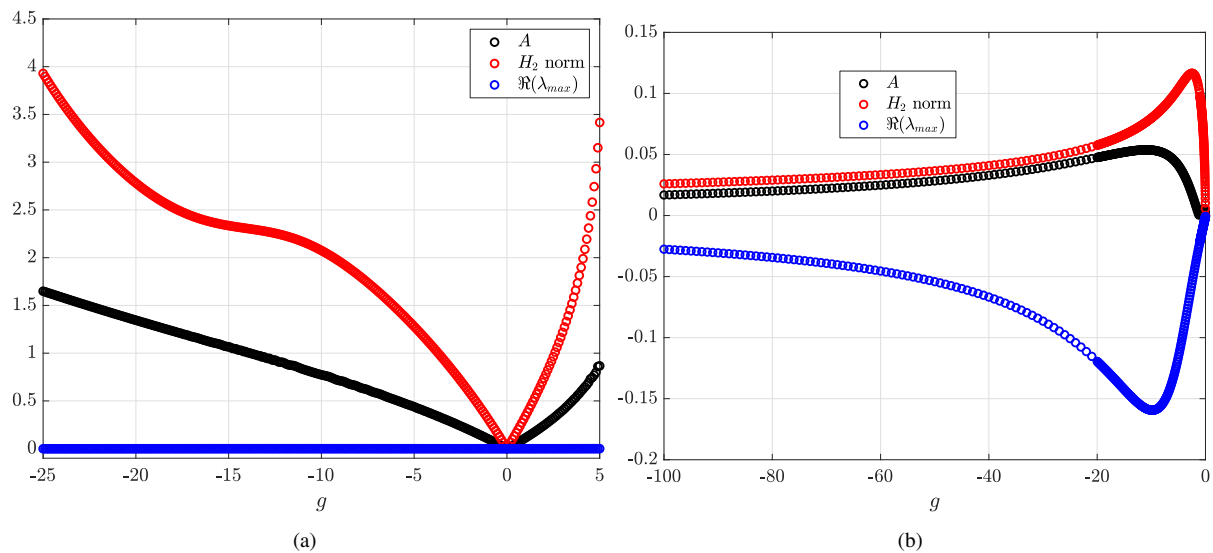


Figure 5: Performance (a) varying $g_p = g$ with $b = 0.01$ and $g_d = 0$. (b) varying $g_d = g$ with $b = 0.01$ and $g_p = 0$. The figures covers values of gain within the interval I .

Acknowledgments. The authors acknowledge the financial support of the São Paulo Research Foundation (FAPESP) through grants #2018/15894-0 and #2021/05140-1 and the National Council for Scientific and Technological Development (CNPq) through grant #305293/2021-4.

Authorship statement. The authors hereby confirm that they are the sole liable persons responsible for the authorship of this work and that all material that has been herein included as part of the present paper is either the property (and authorship) of the authors or has the permission of the owners to be included here.

References

- [1] L. Fok, M. Ambati, and X. Zhang. Acoustic metamaterials. *MRS bulletin*, vol. 33, n. 10, pp. 931–934, 2008.
- [2] M. I. Hussein, M. J. Leamy, and M. Ruzzene. Dynamics of phononic materials and structures: Historical origins, recent progress, and future outlook. *Applied Mechanics Reviews*, vol. 66, n. 4, 2014.
- [3] E. J. Bergholtz, J. C. Budich, and F. K. Kunst. Exceptional topology of non-hermitian systems. *Reviews of Modern Physics*, vol. 93, n. 1, pp. 015005, 2021.
- [4] C. H. Lee and R. Thomale. Anatomy of skin modes and topology in non-hermitian systems. *Physical Review B*, vol. 99, n. 20, pp. 201103, 2019.
- [5] T. Helbig, T. Hofmann, S. Imhof, M. Abdelghany, T. Kiessling, L. Molenkamp, C. Lee, A. Szameit, M. Greiter, and R. Thomale. Generalized bulk–boundary correspondence in non-hermitian topoelectrical circuits. *Nature Physics*, vol. 16, n. 7, pp. 747–750, 2020.
- [6] L. Xiao, T. Deng, K. Wang, G. Zhu, Z. Wang, W. Yi, and P. Xue. Non-hermitian bulk–boundary correspondence in quantum dynamics. *Nature Physics*, vol. 16, pp. 1–6, 020.
- [7] S. Yao and Z. Wang. Edge states and topological invariants of non-hermitian systems. *Physical review letters*, vol. 121, n. 8, pp. 086803, 2018.
- [8] D. Braghini, L. G. Villani, M. I. Rosa, and de J. R. F Arruda. Non-hermitian elastic waveguides with piezo-electric feedback actuation: Non-reciprocal bands and skin modes. *Journal of Physics D: Applied Physics*, vol. 54, n. 28, pp. 285302, 2021a.
- [9] M. I. Rosa and M. Ruzzene. Dynamics and topology of non-hermitian elastic lattices with non-local feedback control interactions. *New Journal of Physics*, vol. 22, n. 5, pp. 053004, 2020.
- [10] J. C. Budich and E. J. Bergholtz. Non-hermitian topological sensors. *Physical Review Letters*, vol. 125, n. 18, pp. 180403, 2020.
- [11] A. Ghatak, M. Brandenbourger, van J. Wezel, and C. Coulais. Observation of non-hermitian topology and its bulk–edge correspondence in an active mechanical metamaterial. *Proceedings of the National Academy of Sciences*, vol. 117, n. 47, pp. 29561–29568, 2020.
- [12] M. Brandenbourger, X. Locsin, E. Lerner, and C. Coulais. Non-reciprocal robotic metamaterials. *Nature communications*, vol. 10, n. 1, pp. 1–8, 2019.

- [13] Y. Chen, X. Li, C. Scheibner, V. Vitelli, and G. Huang. Realization of active metamaterials with odd micropolar elasticity. *Nature communications*, vol. 12, n. 1, pp. 5935, 2021.
- [14] D. Braghini, L. Vilani, M. I. N. Rosa, and J. Arruda. Nonreciprocal waveguides with periodic feedback. In *Proceedings of the XLII Ibero-American Congress on Computational Methods in Engineering, CILAMCE-PANACM*. ABMEC, 2021b.
- [15] W. K. Gawronski. *Dynamics and control of structures: A modal approach*. Springer Science & Business Media, 2004.
- [16] Y. Jin, W. Zhong, R. Cai, X. Zhuang, Y. Pennec, and B. Djafari-Rouhani. Non-hermitian skin effect in a phononic beam based on piezoelectric feedback control. *Applied Physics Letters*, vol. 121, n. 2, 2022.
- [17] Y. Gao and L. Wang. Nonlocal active metamaterial with feedback control for tunable bandgap and broadband nonreciprocity. *International Journal of Mechanical Sciences*, vol. 219, pp. 107131, 2022.
- [18] W. Zhong, R. Cai, X. Zhuang, T. Rabczuk, Y. Pennec, B. Djafari-Rouhani, and Y. Jin. Reconfigurable localized effects in non-hermitian phononic plate. *Applied Physics Letters*, vol. 122, n. 22, 2023.
- [19] S. Skogestad and I. Postlethwaite. *Multivariable feedback control: analysis and design*. John Wiley & Sons, 2005.